Extended Abstracts of the 2011 International Conference on Solid State Devices and Materials, Nagoya, 2011, pp1355-1356

Embedded Biomimetic Nanostructures for Enhanced Optical Absorption in Thin-Film Solar Cells

Hao-Wei Han[1], Min-An Tsai[3], Yu-Lin Tsai[2], Ping-Chen Tseng[2], Peichen Yu[2,*], Hao-Chung Kuo[2], Chang-Hong Shen[4], Jia-Min Shieh[2, 4], and Shiuan-Huei Lin[3], Chien-Chung Lin[1]

[1]Institute of Photonic System, National Chiao Tung University, Tainan 711, Taiwan
[2]Department of Photonics and Institute of Electro-Optical Engineering, National Chiao Tung University, Hsinchu 30010, Taiwan, R. O. C.
[3]Department of Electro-physics, National Chiao Tung University, Hsinchu 30010, Taiwan, R. O. C.
[4]National Nano Device Laboratories No. 26, Prosperity Road 1, Hsinchu 30078, Taiwan
*Phone: +886-3-5712121ext.56357 E-mail: yup@faculty.nctu.edu.tw

1. Introduction

Hydrogenated amorphous silicon (a-Si:H) based thin film solar cells are attractive candidates for large-scale photovoltaics due to their materials being highly abundant on earth and their compatibility for roll-to-roll processing [1]. The mismatch of light absorption depth and minority diffusion length can cause insufficient absorption or carrier collection losses. As a result, efficient light management by reducing the surface reflection as well as increasing the optical path for low energy photons is important for efficiency improvements and cost reduction. Recently, biomimetic antireflective nanostructures have offered a new approach for suppressing the Fresnel reflection. Due to the spatially graded structural profile in a single layer, the nanostructures not only exhibit broadband and omnidirectional antireflective characteristics, but also polarization insensitivity [2]. In this work, we demonstrate an embedded biomimetic nanostructure (EBN) incorporated into a-Si:H solar cells. The semi-oval shaped EBN exhibits antireflective and light trapping effects comparable to an industrial standard cell using an Asahi U glass substrate.

2. Fabrication

The fabrication of the EBN is based on the colloidal lithography and the reactive-ion etching (RIE) technique. First, the silicon nitride (SiN_x) of 380 nm was deposited on a glass substrate by using plasma-enhanced chemical vapor deposition (PECVD). Then the polystyrene (PS) nanospheres was spun on the surface of the SiN_x layer, forming a close-packed monolayer mask. Next, inductively coupled plasma reactive ion etching (ICP-RIE) with incident oxygen (O) plasma was performed to shrink the size of the PS spheres, in order to facilitate the following SiN_x etching processes. The remaining PS nanospheres were removed by dipping into acetone with vibration for 5 min (see Fig. 1(a)). A typical single junction a-Si:H solar cell was then deposited on the substrate, which consists of an 80-nm-thick indium tin oxide (ITO) layer as both top electrode, a 292-nm-thick a-Si:H active layer (p-i-n, 12/260/20 nm), an 80-nm-thick ITO layer as the back electrode, and a 500-nm-thick Al as a back reflector. The schematic is shown in the chart (see Fig. 1(b)-(d)). One flat and one Asahi-U type reference wafers were prepared at the same time with the same procedures. Figures 2(a) show the scanning electron microscopic (SEM) images of the fabricated biomimetic nanostructure. The EBN exhibits a periodicity of 600 nm in a hexagonal close-packed (hcp) lattice. Figure 2(b) shows a cross-sectional transmission electron microscopic (TEM) image of the fully fabricated solar cell on the EBN patterned substrate.

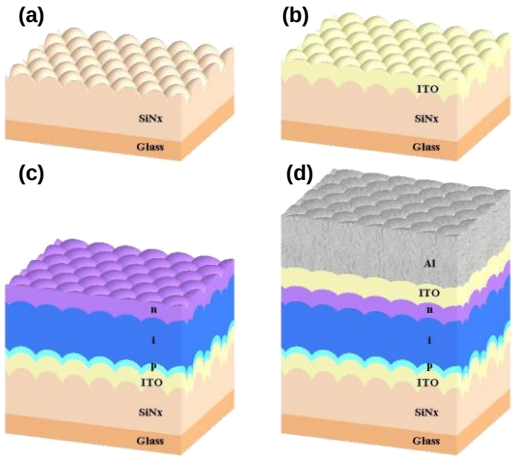

Fig. 1 The schematic fabrication flow for a-Si solar cell with an embedded biomimetic nanostructure (EBN).

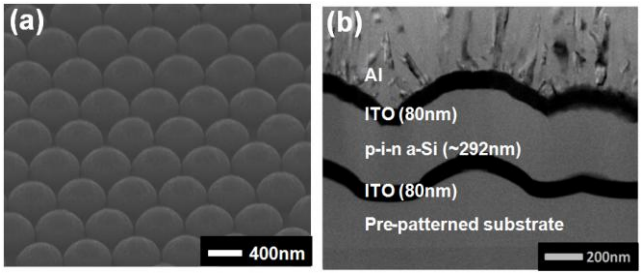

Fig. 2 (a) SEM images of top view. (b) The cross-sectional TEM image of a fabricated solar cell on the EBN-patterned substrate.

3. Results and discussions

Figure 3 shows the reflectance spectra of fabricated cells, which were measured with an integrating sphere at normal irradiance incidence. The reduction is particularly evident in the long wavelength range due to light trapping improvement, which increase the device absorption. More-

over, in the short wavelength range, the EBN cell shows better antireflection than the Asahi U cell. The antireflection effect arises from the tapered structural profile of the EBNs which buffers the index difference between air and dielectric layers.

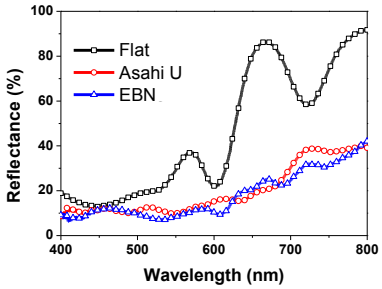

Fig. 3 The reflectance spectra for solar cells deposited on flat, Asahi U glass, and EBN patterned substrates.

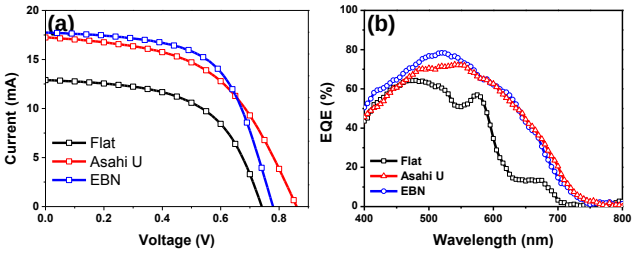

Fig. 4 (a) The current-voltage (I–V) and (b) external quantum efficiency (EQE) characteristics.

The I-V measurement was performed under a simulated AM1.5G illumination condition at room temperature following standard calibration and measurement procedures. As shown in Fig. 4(a), the EBN cell shows improved short-circuit photocurrent J_{sc}=17.74 mA/cm^2, and power conversion efficiencies η=8.32% over the flat thin-film device (J_{sc}=12.89 mA/cm^2 and η=5.36%) made under otherwise identical conditions. The photocurrent and efficiency of the EBN cell is also slightly better than the Asahi U cell (J_{sc}=17.24 mA/cm^2, η=7.70%). On the other hand, the respective open-circuit voltage V_{oc} of the EBN and flat devices are decreased by 0.06 and 0.08 eV from 0.86 eV of the Asahi U cell. The reduction in V_{oc} results from the ITO degradation caused by high-density hydrogen plasma during the deposition of a-Si:H [3]. However, the commercial Asahi U glass substrate uses fluorine-doped tin dioxide (SnO2:F) which is rather resistive to plasmonic damage. Therefore an EQE analysis was carried out to identify the origins of the photocurrent difference. Figure 4(b) reveals that the EBN cell exhibits a higher EQE than the Asahi U for wavelengths less than 560 nm, indicating that the photocurrent improvement mainly occurs in the short wavelength range. Because the required absorption length of a-Si can be estimated, light trapping is only required for λ >= 620 nm. Accordingly, the EQE enhancement before the 620 nm wavelength is attributed to the suppression of optical reflection, while the enhancement after 620 nm can result from mixed contributions of antireflection and light trapping. Figures 5(a) and 5(b) present the calculated enhancement factors of EQE of textured cells with respect to the flat control cell for wavelengths below and above 600 nm, respectively, where the enhancement factor is defined as $EQE=EQE/EQE_{Flat}$.

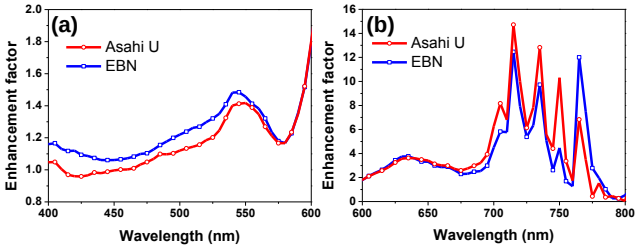

Fig. 5 The improvement factors of the EQE (ΔEQE) for EBN and Asahi U, (a) between 400 nm and 600 nm, and (b) between 600 nm and 800 nm.

4. Angular absorption

Finally, the incident-angle-dependent absorption properties are also critical to solar cells due to the sun movement. Here, we employed angle-resolved absorption spectroscopy to characterize the solar cells. Figures 6(a) and 6(b) show the angular absorptive spectra for solar cells grown on flat and EBN-patterned substrates, respectively. From the absorption color maps, it can be clearly seen that the EBN cell exhibits less dependency on wavelengths and incident angles than the flat cells.

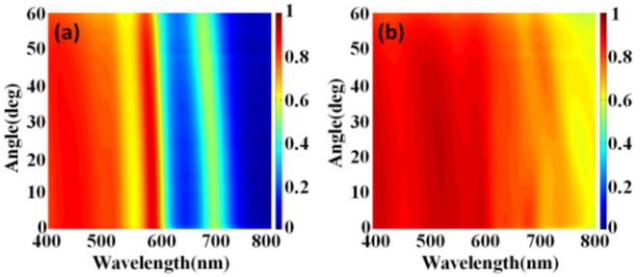

Fig. 6. The measured angular absorption spectra for solar cells deposited on (a) flat and (b) EBN-patterned substrates.

5. Conclusion

We demonstrated the superior antireflection and light trapping properties of an embedded biomimetic nanostructure incorporated into an a-Si:H thin film solar cell. The cell exhibits a higher power conversion efficiency and photocurrent than those obtainable from cells fabricated on flat and commercially available Asahi U substrates. The fabrication of the nanostructure is enabled by scalable polystyrene colloidal lithography, followed by a reactive-ion etching technique. The resulting light management effects directly enable high-efficiency a-Si:H solar cells.

References

[1] D. E. Carlson, C. R. Wronski, Appl. Phys. Lett. **28** (1976) 671-673.

[2] Y.-J. Lee, D. S. Ruby, D. W. Peters, B. B. McKenzie, and J. W. P. Hsu, Nano Lett. **8** (2008) 1501–1505

[3] L. Raniero, I. Ferreira, A. Pimentel, A. Goncalves, P. Canhola, E. Fortunato and R. Martins, Thin Solid Films **511-512** (2006) 295-298